Mat. Res. Bull., Vol. 25, pp. 623-630, 1990. Printed in the USA.
0025-5408/90 $3.00 + .00

CATION DISTRIBUTION AND CHEMICAL DEINTERCALATION OF $Li_{1-x}Ni_{1+x}O_2$

J. Morales, C. Pérez-Vicente, and J.L. Tirado
Departamento de Química Inorgánica e Ingeniería Química. Facultad de Ciencias.
Universidad de Córdoba. 14004 Córdoba. Spain.

(Received February 12, 1990; Communicated by P. Hagenmuller)

ABSTRACT

Cation distribution in $Li_{1-x}Ni_{1+x}O_2$ was studied by Rietvelt analysis of XRD data. The occupancy levels of 3a and 3b sites by Ni and Li atoms approach as x increases, leading to a statistical distribution for $x \geq 0.4$. Acid treatment of these oxides causes the solid to be partly dissolved. The remaining oxide shows divergences in chemical composition and XRD patterns which can be associated with lithium deintercalation. This process is accompanied by a decrease in the rhombohedral angle, α. The thermal behaviour of acid-treated samples is characterized by the occurrence of a spinel phase at ca. 270°C.

MATERIALS INDEX: oxides, lithium, nickel

Introduction

Precise knowledge about the structure and reactivity of lithium/transition-metal mixed oxides with layered, NaCl-related, structures has been gathered in recent years, as a result of the interest in their intercalation-deintercalation and ion-exchange chemistry. In the stoichiometric $LiMO_2$ phases (M: V, Cr, Co and Ni), alternate layers of Li and M cations occupy the octahedral sites of a compact cubic packing of oxide anions, making up a rhombohedral structure with a $R\bar{3}m$ space group, Li in 3b, M in 3a and O in 6c sites (1). In addition, non-stoichiometric phases preserving the layered structure can be obtained by chemical and electrochemical delithiation processes (2-5).

On the other hand, non-stoichiometric phases in a wide compositional range can be obtained by conventional ceramic synthetic methods. This has been shown for the Li-Ni-O system, the preparation conditions of which have a direct effect on the composition of oxides with a $Li_{1-x}Ni_{1+x}O_2$ stoichiometry (5,6). However, the cation distribution in these phases has not yet been examined, although the limiting cases $LiNiO_2$ ($R\bar{3}m$) and $Li_xNi_{1-x}O$ ($x \leq 0.3$) (5,7) (random cation distribution, $Fm\bar{3}m$, NaCl structure) and NiO pseudocubic (NaCl structure) have been accurately characterized.

The Rietvelt method for estimation of cation distributions from powder diffraction data has been successfully applied to various systems (8,9,15). Although the low scattering power of lithium does not allow the precise refinement of Li-positions from X-ray data, the differences in scattering powers of Li and Ni can be exploited to gain a better understanding of the structural variations found in $Li_{1-x}Ni_{1+x}O_2$ phases.

On the other hand, the electrochemical lithium deintercalation in $LiNiO_2$ yields the metastable phase $Li_{0.5}NiO_2$, which is transformed into the normal cubic spinel phase $Li[Ni_2]O_4$ above 200°C (5). By contrast, the chemical delithiation and lithium exchange properties of rhombohedral $LiNiO_2$ have not been reported so far. Moreover, the marked lack of stoichiometry of this mixed oxide (6) may play an important role in the composition and structure of the products of Li-extraction reactions. This paper reports a study on the structure and chemical deintercalation reactions of $Li_{1-x}Ni_{1+x}O_2$ samples.

Experimental

Two Li/Ni mixed oxide samples were prepared by the conventional ceramic procedure by annealing mixtures of Ni(II) hydroxycarbonate and lithium carbonate at 875°C for 18 h under a constant O_2 flow-rate. The products were washed with absolute ethanol, dried at 100°C and stored in a vacuum desiccator with P_4O_{10}. The HCl treatment was carried out by adding 100 ml of 1:50 v/v 36 % HCl to 2.5 g of sample and stirring the mixture at 25°C for 20 h. The solid products were isolated by filtration, washed with distilled water, dried at 100°C and stored in a desiccator.

The average oxidation state of Ni was determined by adding 10 ml of 0.1 M Fe(II), 10 ml of 96 % H_2SO_4 and 10 ml of 85 % H_3PO_4 to 40-60 mg of sample while passing an Ar stream. The solution was back-titrated with standard 0.02 M $K_2Cr_2O_7$ using diphenilamine as indicator. Total Ni content was titrated with 0.1 M EDTA after dissolution of similar amounts of sample in concentrated HCl and neutralization with NH_4OH. Li/Ni ratios were determined by atomic absorption spectrometry.

XRD patterns were obtained on a Siemens D500 diffractometer using CuKα radiation and a graphite monochromator. Step-scan recordings at 0.05°2θ step sizes and 8 s counting times were used in the Rietveld analysis, which was implemented by a computer program described elesewhere (10).

IR data were obtained on a Perkin-Elmer 599A spectrophotometer. TG traces were recorded on a Cahn 2000 electrobalance at 10°C/min heating rate under a static air atmosphere. Transmission electron micrographs were recorder on a JEOL 200 CX microscope.

Results and Discussion

The various samples prepared at 875°C under different O_2 flow-rates were obtained as dark-grey powders with XRD patterns ascribable to a single phase with a $LiNiO_2$-related structure (6) (Fig. 1 A and B). No extra reflections resulting from structural changes or the presence of impurities were detected. Washing the samples with ethanol thus removed undesirable lithium compounds which might interfere with the determination of the chemical composition and the structural refinement.

On the other hand, a comparison of the relative intensities of the reflections with those of stoichiometric $LiNiO_2$ revealed significant divergences. These can be ascribed to structural changes and/or preferred

TABLE I
Li/Ni ratio, average oxidation state (OS) of Ni and stoichiometry of samples A, A1, A2, B and B1.

Sample	Li/Ni	OS	Stoichiometry
A	0.85	2.85	$Li_{0.92}Ni_{1.08}O_2$
A1	0.60	3.10	$Li_{0.65}Ni_{1.08}O_2$
A2	0.30	3.41	$Li_{0.32}Ni_{1.08}O_2$
B	0.52	2.52	$Li_{0.68}Ni_{1.32}O_2$
B1	0.44	3.00	$Li_{0.51}Ni_{1.16}O_2$

orientation phenomena. The layered structure of $LiMO_2$ phases commonly results in a plate-like habit normal to the [001] in the particles of powdered samples of these solids (11,12). However, the electron microscopic images of the samples (Fig. 2) showed these to have little tendency to form regular plates, and several preferred zone axes besides [001] were observed. In addition, changes in particle width were evidenced by the different contrast observed at the particle surfaces. From these data, the effect of preferred orientation may not be a determining factor affecting the intensities of the XRD patterns. Moreover, the samples were prepared so as to minimize these effects.

Table I (A and B) lists the chemical compositions of selected samples. It is worth noting that the observed average oxidation state of Ni is lower than expected for stoichiometric $LiNiO_2$. A direct reationship between the O_2 flow-rate used during the preparation and the observed oxidation state is also found. Oxidation states close to 2.48 have been reported (6) to arise from the temperature of preparation. In our experimental procedure, the different oxidation states were obtained by changing the O_2 flow-rate during the process between 100 ml min^{-1} (sample B) and 200 ml min^{-1} (sample A) at 875°C. The Li/Ni ratios of these samples (Table I) are consistent with the average oxidation state of Ni (OS) (OS = 2 + Li/Ni). Thus, a stoichiometry such as $Li_{1-x}Ni_{1+x}O_2$ is consistent with the above results.

As the Ni/O ratios in these samples are higher than 0.5, cation distribution in these non-stoichiometric samples should allow for the presence of Ni atoms in positions different from the 3a set of the $R\bar{3}m$ s.g.. On the other hand, Li/O ratios lower than 0.5 imply that the 3b equivalent positions are not fully occupied by lithium. Thus, a partial occupation of 3b sites by nickel may be admitted. This is consistent with the tendency of Ni(II), Ni(III) and Ni(IV) ions to occupy octahedral and tetragonally distorted octahedral sites.

A cation distribution of the type $[Li_{1-x}Ni_x]_{3b}[Ni]_{3a}[O_2]_{6c}$ should not have too marked an effect on the unit cell parameters of the rombohedral solid. For x = 1, the resulting solid is NiO, with a NaCl structure. Thus, the unit cell parameter of pseudocubic NiO converted to a rombohedral unit cell with the same number of oxygen layers as the unit cell of $LiNiO_2$ leads to a = 5.907 Å and α = 60°, while rombohedrally distorted NiO yields a = 5.904 Å and α = 60.075° (13). These values are close to those found for stoichiometric $LiNiO_2$ (a = 5.781 Å, α =59.72) (6). However, changes in layer occupancy have a direct effect on the X-ray intensity ratios. These changes are specially evident for the I_{003}/I_{104} ratio, as the 104 ($R\bar{3}m$) or 400 ($Fm\bar{3}m$) line is

TABLE II
Results of the structural refinement of samples A, A1, B and B1, by Rietveld analysis.

Sample	R_P / R_B / R_E	U / V / W	η	Cell Parameters a_R/Å	Cell Parameters α_R/°	$z_{ox.}$	Occupancy Ni {3a / 3b}	Occupancy Li {3a / 3b}
A	6.68% / 2.64% / 3.26%	0.21 / -0.14 / 0.08	0.46	5.787	59.78	0.257_9	1.00 / 0.08	0.00 / 0.92
B	5.32% / 1.31% / 3.37%	0.58 / -0.65 / 0.26	0.37	5.815	59.93	0.258_6	0.92 / 0.40	0.08 / 0.60
A1	7.83% / 3.14% / 3.60%	0.48 / -0.38 / 0.11	0.55	5.800	59.35	0.257_6	1.00 / 0.08	0.00 / 0.65
B1	7.92% / 3.39% / 3.45%	0.57 / -0.37 / 0.17	0.40	5.810	59.21	0.258_6	0.92 / 0.24	0.00 / 0.51

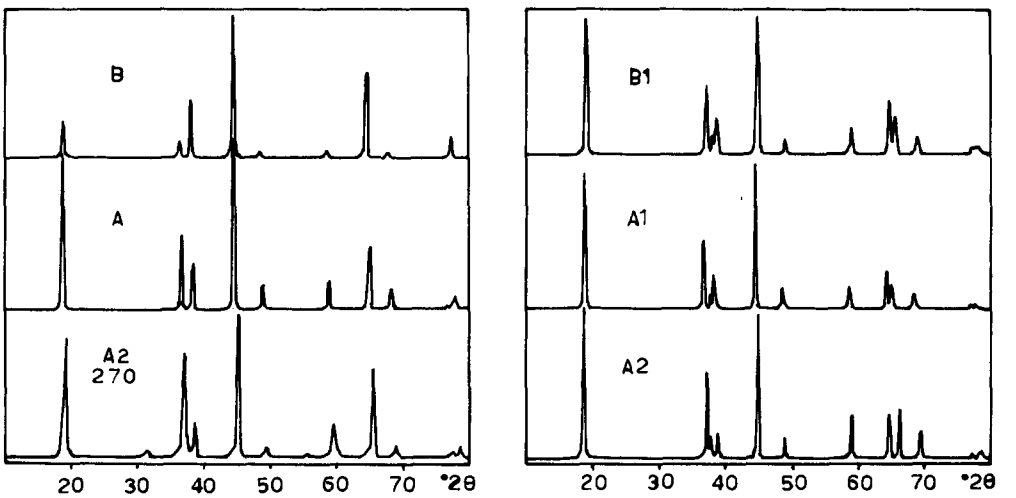

FIG. 1
X-Ray diffraction paterns of samples B, B1, A, A1, A2 and A2-270 measured at λ = 1.54184 Å (CuKα radiation), from 10 to 80° (2θ).

intense in both limiting structures, while 003 ($R\bar{3}m$) or 111 ($Fm\bar{3}m$) should not be observed in the cubic structure. Figure 3 shows the plot of calculated I_{003}/I_{104} ratios vs. the Li/Ni ratio obtained by assuming the above described structural model. The experiental values obtained for sample A are quite consistent with this model.

The Rietveld analysis of XRD data for sample A reveals good agreement between the experimental profile and the structural model, as evidenced by the low R values (Table II). It is worth noting that G_{001} is 0.0 for both samples, thus indicating the absence of preferred orientation phenomena. The values of η (Table II) show that the profiles are accurately described by pseudo-Voigt functions with a similar Gauss and Lorentz contribution. U, V and W show a low broadening of the profiles due to the enhanced sample crystallinity resulting from the application of the ceramic method.

The values of the structural parameters a_R, α_R and z_O (hexagonal), shown in Table II, are intermediate between those found for $LiNiO_2$ and NiO, in agreement with the partial filling of the 3b sites of the rhombohedral structure with Ni ions. α_R is closer to 60° and z_O to 0.25 than in stoichiometric $LiNiO_2$. These results imply that $Li_{1-x}Ni_{1+x}O_2$ oxides with $x < 0.1$ differ from stoichiometric $LiNiO_2$ in the partial substitution of Li by Ni in the interlayer region.

For sample B, with a Li/Ni ratio lower than sample A, Fig. 3 shows a significant divergence from this model. The Rietveld analysis showed poor fitting of the experimental XRD profile. However, if a fraction of Ni atoms in the 3a sites is substituted by Li atoms, different curves can be obtained by plotting I_{003}/I_{104} vs. Li/Ni (Fig. 3). For 8 % substitution, the agreement with the experimental value for sample B is somewhat better. Thus, the Rietveld analysis was carried out from a starting structural model of the type: $[Li_{0.08}Ni_{0.92}]_{3a}[Li_{0.60}Ni_{0.40}]_{3b}[O_2]_{6c}$. This model is intermediate between the proposed structure for sample A and $Li_xNi_{1-x}O$ ($Fm\bar{3}m$) for $x < 0.1$ (7), for which a random distribution of cations was observed in both octahedral layers.

The results of the Rietveld refinement of sample B, shown in Table II, reveal good agreement with this model. Again, the structural parameters a_R, α_R and z_O (hexagonal) are intermediate between those of stoichiometric $LiNiO_2$ and NiO, but closer to those of the latter phase than to those of sample A. From these results can be concluded that large x values in the general formula of the non-stoichiometric phases lead to a distribution of Li and Ni ions in both sets of octahedral sites with a marked tendency to a statistical cation distribution (NaCl-type structure).

The room temperature treatment of A and B samples with HCl resulted in partial dissolution, accompanied by Cl_2 release, consistent with earlier reports (6). The solid products form this treatment showed changes in the chemical composition (see Table I) and XRD patterns (Fig. 1). The Li/Ni ratios decreased gradually with the reaction time (see A, A1 and A2), thus indicating the occurrence of lithium extraction or a proton exchange reaction. The possibility that a Li^+/H^+ exchange may take place was examined by recording the IR spectra of the diferent samples. As in $LiNiO_2$ (1), no absoption effects were detected in the 4000-1600 cm^{-1} frequency range, in contrast with $HCoO_2$, (isostructural with $LiNiO_2$) which shows a broad IR absoption band at ca. 1800 cm^{-1} (14). In addition, any proton exchange should lead to a marked decrease in the unit cell c_H parameter, as found in $LiCoO_2/HCoO_2$ (11) and $LiCrO_2/HCrO_2$ (12), or complex structural changes leading to spinel-type phases as found in α-$LiAlO_2$ (15). None of these effects were detected in our samples, which thus

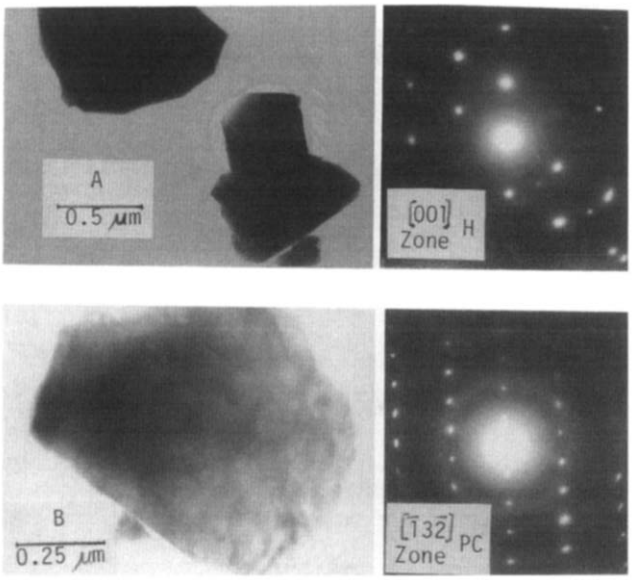

FIG. 2
Electron micrographs of samples A and B showing $[001]_h \equiv [111]_{pc}$ and $[\bar{1}3\bar{2}]_{pc}$ zone axis (h: hexagonal, pc: pseudo-cubic $\alpha_R = 60°$).

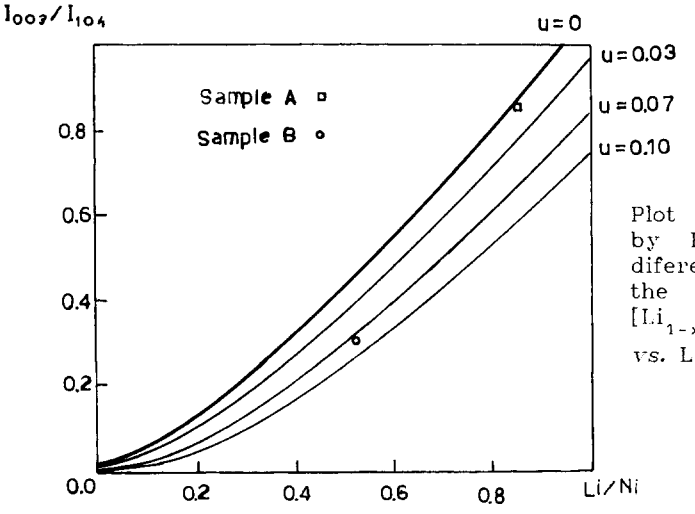

FIG. 3
Plot of I_{003}/I_{104}, calculated by Rietveld simulation for diferent u values, based on the cation distributions $[Li_{1-x-u}Ni_{x+u}]_{3b}[Li_uNi_{1-u}]_{3a}$, vs. Li/Ni ratio.

confirmed the absence of exchange phenomena.

On the other hand, as can be seen in Table I, the average Ni oxidation state increases gradually with the length of the HCl treatment. This can be related with the above mentioned delithiation process. The experimental Li/Ni and Ni(OS) values can be summarized in the chemical compositions, also shown in Table I, by assuming the initial oxygen packing to remain unaltered. From these formulae, it is worth noting that sample B has decreased Ni/O and Li/Ni ratios. This may be interpreted in terms of a loss of interlayer Ni ions (in addition to Li^+) throughout the HCl treatment. After equal reaction times, the Ni/O ratios are similar (compare A1 with B1), while further treatment of the A1 sample affects the Li/Ni ratios exclusively.

These results allow the reactions induced by the HCl treatment to be derived. First, the chemical delithiation caused by the acid treatment could be written independently of the observed Cl_2 release as:

$$2(1-x+y)\ Li_{1-x}Ni_{1+x}O_2 + 8y\ H^+ \rightarrow 2(1-x)\ Li_{1-x-y}Ni_{1+x}O_2 + \\ + 2y(1+x)\ Ni^{2+} + 3y(1-x)\ Li^+ + 4y\ H_2O \qquad [1]$$

A Ni(III) dismutation reaction was also observed in the hydrolysis of $NaNiO_2$ in a basic medium and in a 1 M NH_4Cl medium. An γ-oxyhydroxide with a Ni oxidation state higher than 3 occurred in the absence of oxidants (16). The dissolution reaction in the HCl medium may take place simultaneously with Cl^- ions being oxidized by Ni(III) according to:

$$2(1+x)\ Li_{1-x}Ni_{1+x}O_2 + 2(1-x)\ Cl^- + 8(1+x)\ H^+ \rightarrow \\ \rightarrow 2(1+x)^2\ Ni^{2+} + 2(1-x^2)\ Li^+ + (1-x)\ Cl_2 + 4\ H_2O \qquad [2]$$

Reactions [1] and [2] are not quantitatively combined. For sample B, and according to the results listed in Table I, the process involves the deintercalation of Ni ions concomitantly with the delithiation. The process can be then formulated as:

$$Li_{0.68}Ni_{1.32}O_2 + 0.04\ Cl^- \rightarrow Li_{0.51}Ni_{1.16}O_2 + 0.17\ Li^+ + \\ + 0.16\ Ni^{2+} + 0.02\ Cl_2 \qquad [3]$$

The X-ray diffraction patterns of deintercalated samples A1 and B1 were used to study cation distribution in these products by the Rietveld method. Table II lists the parameters values obtained and the R coefficients. For sample A1, the best fitting was achieved by assuming a loss of Li^+ ions from the 3b sites exclusively during the deintercalation of sample A. For sample B1, Li^+ ions were removed from 3a and 3b sites, while nickel was removed form 3b as a result of the above mentioned Ni,Li extraction. The occupancy factors derived from these assumptions and the chemical compositions are listed in Table II. The refined rhombohedral unit cell parameters α_R for A1 and B1 are more divergent from 60° than in the untreated samples A and B. This can account for the differences in the number of reflections shown in the X-ray diffraction patterns in Fig. 1 as 222-200 and 422-2$\bar{2}$0 are coincident for $\alpha_R = 60°$ (222 and 440 of the cubic unit cell). This change is also consistent with the preferential ion extraction from 3b sites, thereby increasing the rhombohedral distortion from the limiting cubic structure case, a behaviour which is also observed in electrochemically delithiated $LiNiO_2$ (5).

As a final proof of the chemical delithiation process, we studied the thermal behaviour of the delithiated sample with Li/Ni ratio close to 0.5 (sample A2). After treating this sample at 120°C for 1 h, the XRD pattern of the resulting sample (Fig. 1) showed lines ascribable to a structure with $\alpha_R = 60°$. In addition, a diffraction line ascribable to the (220) planes was also observed. This line is characteristic of a $Fd\bar{3}m$ cubic spinel structure, such as that found in the thermal treatment of $Li_{0.5}NiO_2$ at the same temperature (5).

Conclusions

$Li_{1-x}Ni_{1+x}O_2$ can be synthesized over a wide compositional range by changing the O_2 flow-rate used in the process. The non-stoichiometry of these oxides results in a cation distribution intermediate between $LiNiO_2$ (all Li atoms in 3b and Ni in 3a sites $R\bar{3}m$ s.g.) and $Li_xNi_{1-x}O$ (statistical distribution of Li and Ni in 3a and 3b sites).

A partial dissolution of the solid with Cl_2 evolution is observed by treating the non-stoichiometric oxides with 0.6 M HCl. Simultaneously to this reaction, a lithium deintercalation process is also observed. The resulting solid features a higher average oxidation state of Ni and a lower Li/Ni ratio and rhombohedral α parameter than the starting sample. Cation distribution in deintercalated samples is similar to that found in electrochemically deintercalated $LiNiO_2$.

Acknowledgement

The authors acknowledge financial support from CICYT and PFPI.

References

1. T.A. Hewston and B.L. Chamberland, J. Phys. Chem. Solids 48, 97 (1987).
2. K. Mizushima, P.C. Jones, P.J. Wiseman and J.B. Goodenough, Mater. Res. Bull 15, 783 (1980).
3. K. Vidyasagar and J. Gopalakrishnan, J. Solid State Chem. 42, 217 (1982).
4. L.A. de Picciotto, M.M. Thackeray, W.I.F. David, P.G. Bruce and J.B. Goodenough, Mater. Res. Bull. 19, 187 (1984).
5. M.G.S.R. Thomas, W.I.F. David and J.B. Goodenough, Mater. Res. Bull. 20, 1137 (1985).
6. L.D. Dyer, B.S. Borie, Jr. and G.P. Smith, J. Am. Chem. Soc. 76, 1499 (1954).
7. H. Taguchi and Y. Takahashi, J. Mater. Sci. 19, 3347 (1984).
8. A.G. Nord, J. Appl. Cryst. 17, 55 (1984).
9. M.M. Thackeray, L.A. de Picciotto, W.I.F. David, P.G. Bruce and J.B. Goodenough, J. Solid State Chem. 67, 285 (1987).
10. D.B. Wiles and R.A. Young, J. Appl. Cryst. 14, 149 (1981).
11. J.M. Fernández-Rodriguez, L. Hernán, J. Morales and J.L. Tirado, Mater. Res. Bull. 23, 899 (1988).
12 L. Hernán, M. Macías, J. Morales, C. Pérez-Vicente and J.L. Tirado, Mater. Res. Bull. 24, 781 (1989).
13. C.J. Toussaint, J. Appl. Cryst. 4, 293 (1971).
14. R.G. Delaplane, J.A. Ibers, J.R. Ferraro and J.J. Rush, J. Chem. Phys. 50, 1920 (1969).
15. K.R. Poeppelmeier and D.O. Kipp, Inorg. Chem. 27, 766 (1988).
16. J.J. Braconnier, C. Delmas, C. Fouassier, M. Figlarz, B. Beaudouin and P. Hagenmuller, Rev. Chim. miner. 21, 496 (1984).